Scale resolving simulations of the water flow through a rod bundle with split-type spacer grid

A A Matyushenko, A V Garbaruk
Saint-Petersburg State Politechnical University
Russia, Saint-Petersburg, 195251, Politechnicheskaya, 29

Abstract. Unsteady isothermal turbulent flow in periodic sub-channel of 5x5 rod bundle with split-type spacer grid is investigated using modern Scale Resolving Simulation methods: Wall Modelling Large Eddy Simulation (WMLES) and Scale Adapting Simulation (SAS). Solutions obtained with both methods show complicated swirling flow dissipating over the distance from spacer grid and are in a good agreement with the experimental data except an area in close vicinity of the vanes.

1. Introduction

Spacer grids with mixing vanes are widely used in pressurized water nuclear reactors for heat transfer enhancement and coolant flow optimization provided for a nuclear fuel assembly. In recent years Computational Fluid Dynamics (CFD) is increasingly used for design of such grids, analysis of complex flow and heat transfer of relevance to nuclear plant safety. From a thermal hydraulic standpoint, accurate prediction of the velocity and turbulence fields in a rod bundle with spacer grids with mixing vanes is a challenging task. In engineering practice, such tasks are usually solved using steady or unsteady Reynolds Averaged Navier-Stokes equations, (RANS or URANS) which are not always capable to predict such complex strong swirling flow. Scale Resolving Simulation (SRS) methods potentially are more effective; however, the experience of their usage for flow through the rod bundle with spacer grids with mixing vanes is not sufficient.

The aim of present work is an assessment of modern SRS methods for prediction of complex swirling flow through rod bundle with split-type spacer grid with the use of ANSYS FLUENT CFD code. CFD analysis is based on experiments performed in the Korea Atomic Energy Research Institute (KAERI) at Measurements & Analysis of Turbulence in Subchannels – Horizontal (MATiS) test facility [1].

2. MATiS-H test facility

The main test section of the MATiS-H test facility consists of a 170x170 mm^2 square channel which contained a 5x5 rod bundle array installed in a horizontal position (Figure 1). For a fine-scale examination of the lateral flow structure in a sub-channel geometry and for increasing of LDA measurement resolution, the size of the 5x5 rod bundle array is enlarged in 2.67 times and comprises of 25 rods of 25.4 mm outer diameter and 4m length in a regular matrix arrangement with a rod pitch of P = 33.12 mm and a wall pitch of 18.76 mm. Consequently, the hydraulic diameter of the channel cross-section, which considers the flow area and the wetted perimeter in a square duct including the 5x5 rod bundle, is D_H = 24.27 mm. Split-type spacer grid is mounted to the rods with the use of so-called “buttons” (small cylinders). The grid can be moved in the axial direction along the 5x5 rod bundle array, in order to perform velocity measurements at different cross sections downstream of the

tips of the mixing vanes of the spacer grid ($0.5D_H$, $1.0D_H$, $4.0D_H$ and $10.0D_H$) based on the test specification, while a measurement cross section remains in a fixed position.

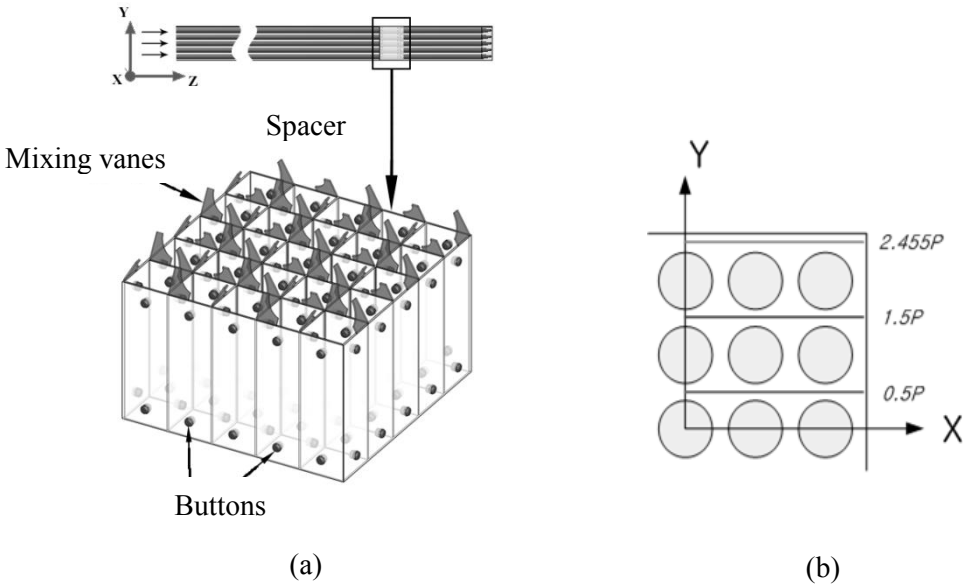

(a) (b)

Figure 1. Scheme of the main section of MATiS-H test facility (a) and location of measurement cross sections (b)

Water at normal pressure and temperature conditions is used for all the MATiS-H experiments. The mass flow rate in all experiments is 24.2 kg/s resulting in a bulk velocity of 1.5 m/s corresponding to the Reynolds number based on the hydraulic diameter of Re = 50250. The water flow enters a lower plenum of the horizontal test section with an installed flow breaker. Then the flow passes two flow straighteners, which are installed in order to homogenize the flow and to accelerate the formation of a fully developed flow in the 5x5 rod bundle. The second of those flow straighteners is installed at a distance of $100D_H$ upstream of the spacer grid. Therefore it is assumed, that flow is fully developed at the inlet section of the spacer grid.

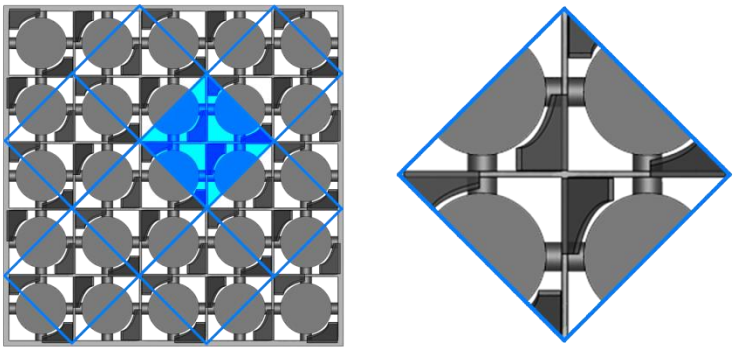

Figure 2. Full configuration of split spacer grid (left) and periodic sub-channel(right)

The most part of the full split-type spacer grid configuration except an area near the duct wall consists of periodic sub-channels (Figure 2). Note that fully periodic flow in the sub-channel should capture all specific features of this flow.

3. Problem definition

A computational domain consists of a section with a length of $4D_H$ located upstream of the spacer grid, the spacer grid itself and a section with length more than $10.0D_H$ downstream of the spacer grid. Topology of the computational domain and applied boundary conditions are shown in Figure 3.

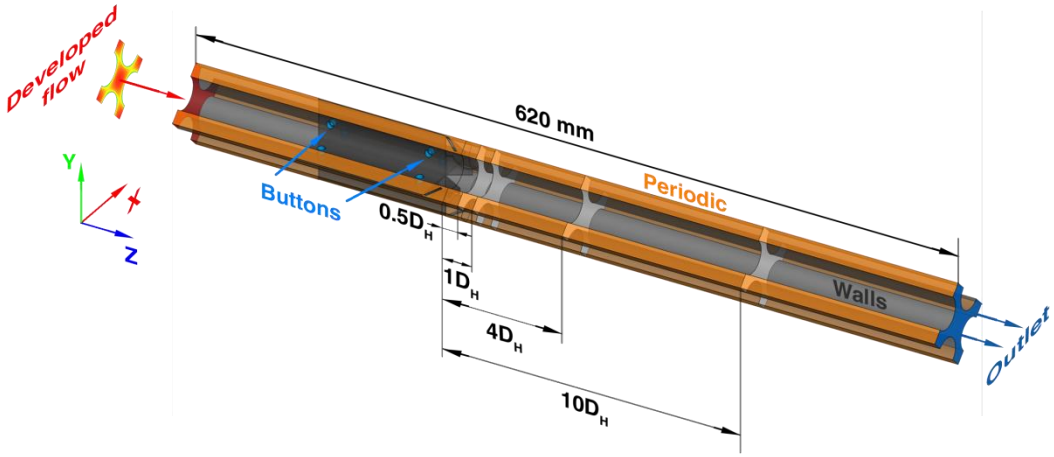

Figure 3. Computational domain

The geometry and a mesh are created with the use of pre-processing applications within the ANSYS Workbench platform (ANSYS Design Modeler and ANSYS Workbench Meshing). The hexahedral mesh is preferable from a CFD accuracy point of view, but it is judged to be less flexible and too expensive to create a high quality mesh. Instead, hybrid meshes are created with the use of ANSYS Workbench Meshing. In the framework of this strategy the flow domain is decomposed into three zones: upstream of the spacers, spacers and downstream of the spacers. At the first stage hexahedral high quality mesh suitable for SRS methods (streamwise and spanwise mesh steps are less than 0.1 of boundary layer thickness) is created in the downstream section. During the second stage tetrahedral mesh with prismatic layers near the walls is built in the spacer grid based on the first stage mesh. Finally upstream mesh is obtained as a sweep of the grid surface at the beginning of the spacer grid. Total mesh parameters are shown in Table 1.

Table 1. Mesh parameters

Number of cells	Max. Y^+	Mean Y^+	Min cell size, mm	Max cell size, mm
40M	5	1.5	0.001	1

Time step of $\Delta t = 0.1$ ms is sufficient to resolve the smallest turbulent structures downstream of the spacer grid (CFL number based on the streamwise grid is of the order of 1).

Water properties at 35°C are specified as a constant property incompressible liquid. SRS methods are performed with the algebraic Wall-Modelling LES (WMLES) [2] model and Scale Adapting Simulation (SAS) [3].

On solid walls automatic near wall treatment is used. Constant static pressure level is specified on the outlet boundary. On the inlet boundary fully developed velocity profiles obtained with the use of SST RANS in combination with Vortex Method (VM) [4] are specified. Other than that, in order to check the influence of the inflow turbulent content on the flow downstream of the spacer grid a SAS computation without VM is also performed.

4. Flow structure

The considered flow through the rod bundle is extremely unsteady. Resolved turbulence upstream of the vanes consists of interaction of the inlet turbulence and a vortex shedding in the wake of the buttons. However, the most significant unsteadiness showed in Figure 4 is provided by the mixing vanes of the spacer grid. Effect of the vanes results in strongly swirling flow in the centre of the sub-channel and in two additional vertices in the rod gap dissipating downstream of the grid (Figure 5).

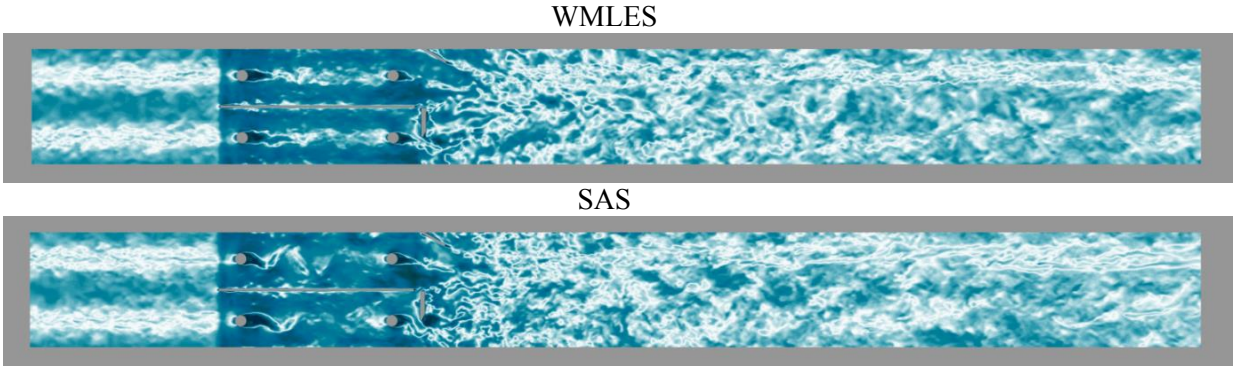

Figure 4. Flow structure visualized by streamwise velocity contours

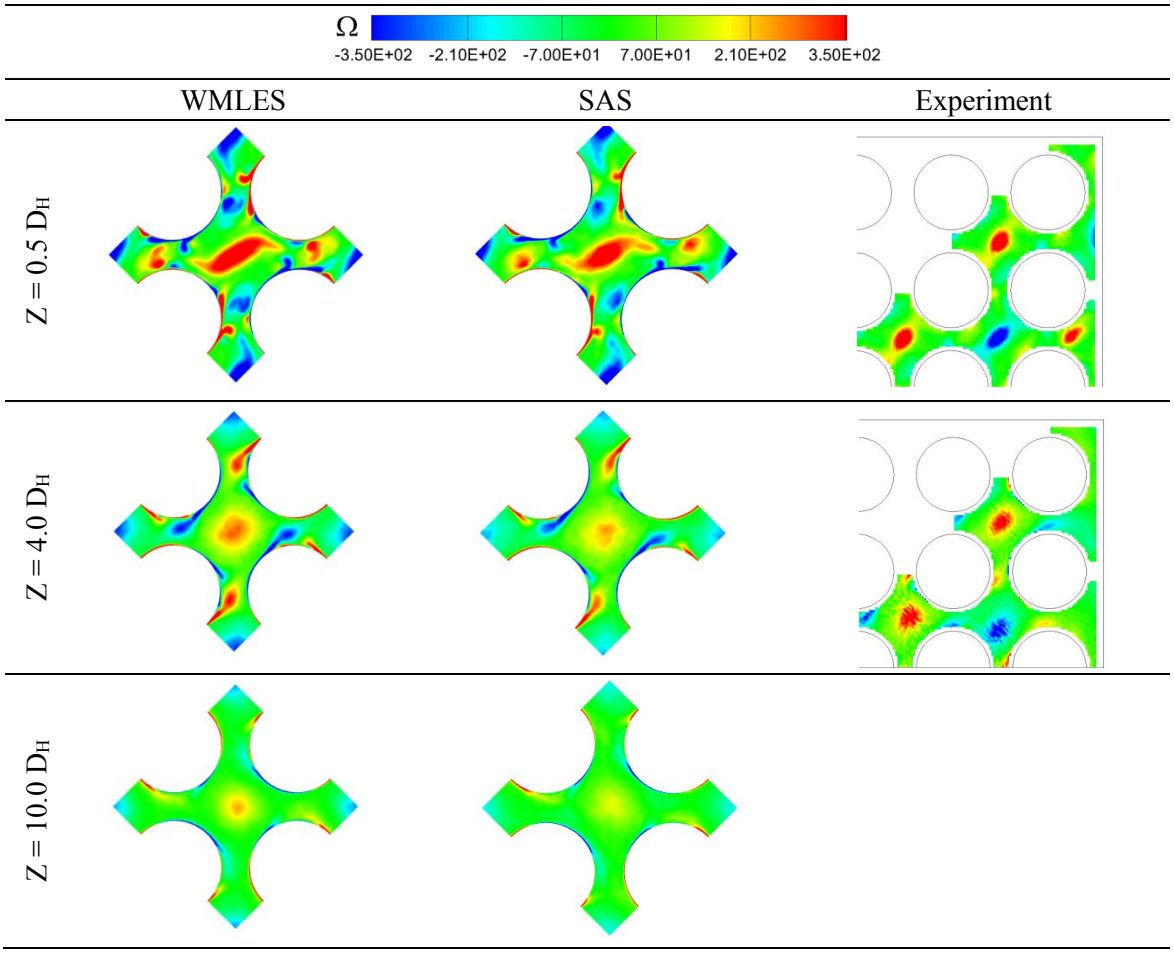

Figure 5. Mean z-vorticity contours for different turbulence models at different sections

5. Comparison of CFD results with experimental data

Time-averaged velocity profiles and turbulence characteristics are compared with the experimental measurements at Y = 0.5P line (Figure 1b) at different cross sections downstream of the spacer grid (Figure 6). Both models predict the main vertices quite well. However, in the nearest section ($Z = 0.5D_H$) there is a visible superiority of SAS over WMLES especially in the level of resolved turbulence. The reason can be in algebraic nature of WMLES. Prandtl model near the walls is used for this method which can be incapable to predict such a complex flow. Further downstream the difference decreases and solutions of both models become similar and correspond to the experimental measurements fairly well.

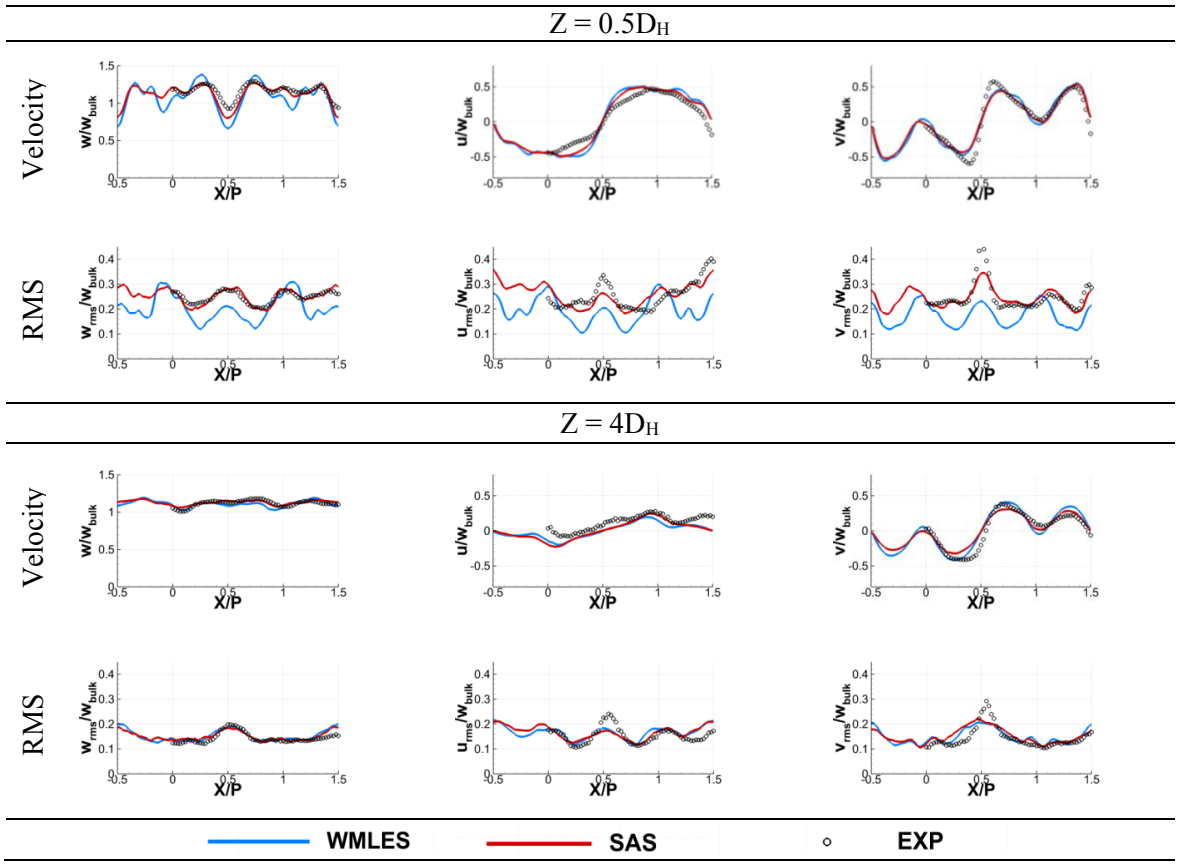

Figure 6.Time-averaged velocity profiles and RMS velocity fluctuations at Y = 0.5P line at different cross sections

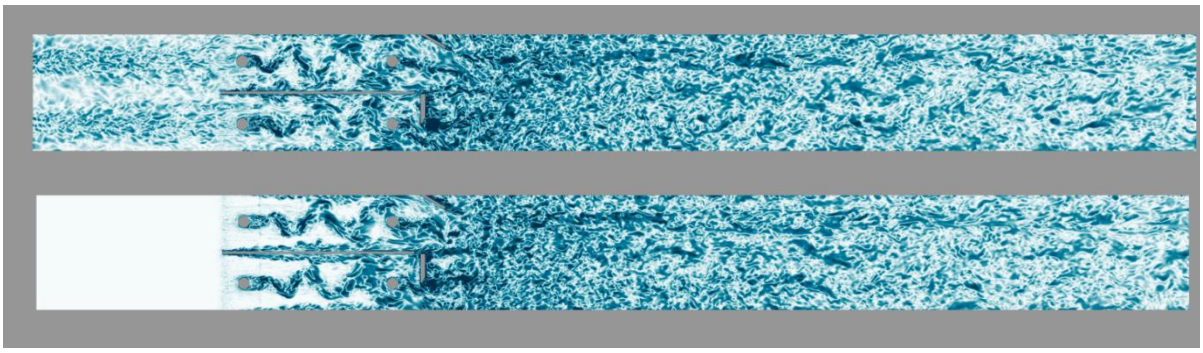

Figure 7. Instantaneous SAS vorticity contours with (top) and without (bottom) inlet turbulent content

6. Influence of inlet turbulent content

An effect of turbulent content specification at the inlet section on vorticity fields is shown in Figure 7. Turbulent structures created by VM have an influence on the flow before and inside the spacer grid. However, downstream of the mixing vanes turbulent structures are very similar for both types of boundary conditions. Comparison of time-averaged characteristics at $Z = 0.5D_H$ section near the mixing vanes (Figure 8) shows similar results for both computations. So, the tubulisation by the mixing vanes does not depend on presence of inlet turbulence.

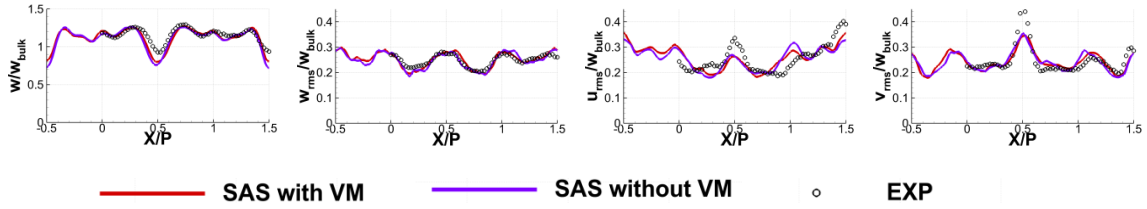

Figure 8. Time-averaged and RMS velocity profiles at $Y = 0.5P$ line at $Z = 0.5D_H$ section

7. Conclusions

The flow through the periodic sub-channel of the rod bundle array with split-type spacer grid has been investigated using ANSYS FLUENT. Flow predictions carried out using WMLES and SAS method show unsteady complicated swirling flow dissipating over the distance from the spacer grid with mixing vanes.

Both methods show fairly good agreement with KAERI MATiS-H benchmark data in prediction of main vortex structures. SAS excels WMLES in prediction of streamwise velocity and RMS values of velocity fluctuations near the mixing vanes. However, in the rest downstream sections both methods yield very close solutions which are in a good agreement with the experiment.

Computation with SAS without VM shows that flow and time-averaged characteristics downstream of the spacer grid is insensitive to turbulent content on the inlet boundary. Note, that for this task WMLES requires generation of turbulent content and should not be used without VM.

Acknowledgements

This work is partially supported by the Russian Foundation for Basic Research (grant No. 12-08-00256)

References

[1] OECD/NEA. 2011. MATiS-H Benchmark. *Final Benchmark Specifications, pp. 44.*

[2] Shur M. L., Spalart P. R., Strelets M. K. & Travin A. K. 2008. A hybrid RANS-LES approach with delayed-DES and wall-modelled LES capabilities. *International Journal of Heat and Fluid Flow, 29(6), 1638-1649. Elsevier Inc.*

[3] Menter F. R. & Egorov Y. 2006. SAS turbulence modelling of technical flows. *Direct and Large-Eddy Simulation VI, 687–694.*

[4] Mathey F. 2008. Aerodynamic noise simulation of the flow past an airfoil trailing-edge using a hybrid zonal RANS-LES. *Computers & Fluids, Volume 37, pp. 836–843.*